scientific reports

Check for updates

OPEN

IL-18 promotes pancreatic fibrosis via release of IL-4 from pancreatic stellate cells and induces macrophage M2 polarization

Guangping Tu[1], Cheng Peng[1,2], Shuangxi Xie[1], Shixu Zheng[1], Haibo Jiang[1], Lang Chen[1], Xiao Yu[1] & Zhiqiang Li[1]✉

Chronic Pancreatitis (CP) is a progressive inflammatory disease leading to fibrosis. The role of interleukin-18 (IL-18), an inflammation-associated cytokine, in CP, especially its interactions with pancreatic stellate cells (PSCs) and macrophages, remains unclear. Human CP tissues and caerulein-induced CP models in mice were used to explore the role of IL-18 in fibrosis. Histopathological analysis, immunofluorescence, and in vitro co-culture systems were employed to identify cellular targets and downstream signaling of IL-18. IL-18 expression was elevated in CP pancreata, correlating with the severity of fibrosis. Deletion of IL-18Rα reduced fibrosis, PSC activation, and macrophage M2 polarization in CP mice. IL-18 directly stimulated PSCs to secrete interleukin-4 (IL-4), which induced M2 polarization of macrophages, exacerbating fibrosis. Inhibition of IL-4 alleviated fibrosis and M2 polarization. IL-18 plays a critical role in driving pancreatic fibrosis by modulating PSCs-macrophage interactions, providing a potential therapeutic target to disrupt the fibrotic process in CP.

CP is a progressive disease characterized by persistent inflammation, excessive deposition of extracellular matrix (ECM), and gradual loss of pancreatic function, leading to debilitating symptoms and a markedly increased risk of pancreatic cancer[1–3]. Although CP arises from diverse etiologies, its pathogenesis is primarily driven by sustained and excessive inflammatory responses, which ultimately culminate in pancreatic fibrosis (PF). The transition from inflammation to fibrosis involves complex interactions among multiple immune cell populations, particularly macrophages, and the activation of PSCs[4,5]. These cells play a crucial role in fibrosis by secreting ECM components, thereby promoting fibrotic tissue deposition and structural remodeling of the pancreas.

Inflammasome-associated pathways have been implicated in PF progression[6–8]. Pyroptosis triggers the release of the pro-inflammatory cytokine IL-18, a member of the IL-1 cytokine family, which is produced by macrophages, dendritic cells, and epithelial cells. Canonically, IL-18 binds to its heterodimeric receptor complex (IL-18Rα and IL-18Rβ), activating downstream signaling pathways such as NF-κB and MAPK, which promote the production of pro-inflammatory cytokines, chemokines, and mediators involved in the recruitment and activation of immune cells[9]. IL-18 has been implicated in exacerbating tissue injury and fibrosis[10], suggesting its potential role as a mechanistic link between pyroptosis and PF. Increasing evidence indicates that IL-18 exerts immunomodulatory effects in chronic inflammatory disorders[10–13], with strong associations to macrophages and stellate cells in chronic diseases. In pancreatic disorders, IL-18 expression is markedly elevated in CP tissues and correlates with the severity of fibrosis, indicating its potential as a critical regulator of fibrotic progression[14]. However, the precise mechanisms remain to be clarified. This study focuses on IL-18/IL-18Rα signaling and does not directly examine the pyroptotic execution molecules (GSDMD/GSDME cleavage). Therefore, "pyroptosis" is not considered a directly experimentally confirmed upstream event.

Activation of PSCs represents a central event in the development of fibrosis in CP[15]. Activated PSCs secrete excessive ECM, driving fibrotic deposition. Additionally, PSCs contribute to pancreatic inflammation; secretions from damaged pancreatic acinar cells (PACs) and immune cells (e.g., macrophages, T cells) further promote PSC activation[4]. These activated PSCs exacerbate fibrosis and release cytokines such as IL-33[16] and IL-11[17], perpetuating inflammatory responses and creating a vicious cycle.

Macrophages are key orchestrators of the inflammatory microenvironment in CP, with their polarization status serving as a critical determinant of both inflammatory and fibrotic outcomes[18,19]. The role of IL-18 in macrophage

[1]Department of Hepatopancreatobiliary Surgery, Third Xiangya Hospital, Central South University, Tongzipo Road No.138, Changsha 410013, Hunan, China. [2]Department of Hepatobiliary and Pancreatic Surgery, Hainan Hospital of Hainan Medical College, Hainan 570311 Haikou, China. ✉email: li_zhiqiang6138@163.com

regulation has been well-documented in acute pancreatitis. In severe acute pancreatitis models, infiltrating macrophages promote inflammation while inducing IL-18-mediated Th2 cell responses[20], underscoring their therapeutic potential. IL-4, a pivotal cytokine driving M2 macrophage polarization, is markedly upregulated in CP pancreatic tissues and promotes fibrogenesis[21,22]. Although the cellular source of IL-4 remains incompletely defined, accumulating evidence suggests that PSCs secrete IL-4 during CP, which interacts with macrophages to induce M2 polarization and exacerbate fibrosis[21]. However, the mechanisms underlying IL-4 secretion by PSCs are poorly understood. Furthermore, in vivo studies suggest that IL-18 promotes cardiac and renal fibrosis by modulating M2 macrophage polarization[10,23,24], although the mechanism by which this regulation occurs remains to be elucidated.

Compared to IL-18, its upstream regulator, the NLRP3 inflammasome, has been more extensively investigated in CP[24]. Nevertheless, clarifying the multifaceted role of IL-18 in CP and its contribution to PF may yield valuable insights for developing therapies against this intractable disease. In the present study, we first demonstrated that IL-18 expression in CP patient tissues positively correlates with PF severity, with IL-18 predominantly localized to PACs, whereas IL-18Rα is chiefly expressed on PSCs rather than macrophages. In a murine CP model, IL-18Rα deficiency markedly alleviated PF, suppressed PSC activation, and reduced M2 macrophage infiltration. Mechanistically, we found that IL-18 directly stimulates PSCs to secrete IL-4, and that conditioned medium from IL-18-treated PSCs promotes M2 macrophage polarization. Notably, pharmacological inhibition of IL-4 substantially attenuated this polarization effect. These findings provide new mechanistic insights into the IL-18/IL-4 axis in CP and highlight potential therapeutic targets for preventing the progression of PF.

Materials and methods

Ethics declaration

All animal experiments were approved by the Ethics Committee of the Third Xiangya Hospital of Central South University. This study is performed in accordance with relevant guidelines and regulations. All methods are reported in accordance with ARRIVE guidelines.

All human samples were obtained from Xiangya Third Hospital of Central South University, and informed consent has been obtained from all subjects and/or their legal guardians. All experiments were approved by the Ethics Committee of Xiangya Third Hospital of Central South University(NO 2021-S149) and performed in accordance with relevant guidelines and regulations.

Antibodies and reagents

Caerulein (#HY-A0190) was purchased from MedChemExpress. Primary antibodies: IL-18 (#DF6252), IL-4 (#AF5142), and Collagen I (#AF7001) were purchased from Affinity Biosciences. Amylase (#3796S) and iNOS (#13120) were purchased from Cell Signaling Technology. IL18Rα (#AF856) was purchased from Bio-Techne Corporation. α-SMA (#GB111364) was purchased from Servicebio, Inc. CD206 (#AB64693)was purchased from Abcam Plc. F4/80 (#GB11027) and CD68 (#GB14043) were purchased from Servicebio, Inc. Secondary antibodies: Goat Anti-Rabbit IgG (H + L) HRP(#S0001) was purchased from Affinity Biosciences. HRP conjugated Goat Anti-Rabbit IgG (H + L) (#GB23303), Cy3 conjugated Goat Anti-Rabbit IgG(H + L) (#GB21303), FITC conjugated Donkey Anti-Rabbit IgG(H + L) (#GB22403), FITC conjugated Goat Anti-Mouse IgG(H + L) (#GB22301) were purchased from Servicebio, Inc.

Human pancreatic samples

The samples were collected from patients diagnosed with CP based on imaging and histopathological criteria. Detailed clinical histories, laboratory tests, and imaging data were recorded for each patient. Standard pancreatic tissue samples, used as controls, were sourced from non-CP patients undergoing pancreatic surgery for non-inflammatory conditions.

Animals

C57BL/6J wild-type (WT) mice were obtained from Hunan SJA Laboratory Animal Co., Ltd, and IL-18Rα knockout mice (*Il18Rα*$^{-/-}$) were purchased from the Jackson Laboratory. All experimental mice were age-matched (8–10 weeks old) and weighed 20–25 g. Mice were housed in specific pathogen-free facilities under a 12-hour light/dark cycle with ad libitum access to standard chow and water.

Induction of CP in mice

To establish the CP model, mice were subjected to repeated caerulein injections as previously described[25,26]. Briefly, mice received hourly intraperitoneal injections of caerulein (50 μg/kg) for six consecutive hours, three times a week, over a period of six weeks.

To validate the in vivo role of IL-18 mediated through IL-4, we administered 500 ng of recombinant mouse IL-18 (rmIL-18; #HY-P73181, MedChemExpress) intraperitoneally three times a week, starting two weeks after the initial caerulein injection. To further neutralize IL-4, a concurrent intraperitoneal injection of 0.75 mg Ultra-LEAF™ Purified anti-mouse IL-4 antibody (#504138, BioLegend) was administered on the same schedule, beginning two weeks after the first caerulein injection. Control mice received an equivalent dose of Ultra-LEAF™ Purified Rat IgG1 Isotype Control antibody. To exclude acute-phase effects, all animals were euthanized three days post the final caerulein injection. Mice were anesthetized with sodium pentobarbital (50 mg/kg, i.p.). After confirmation of absent pedal withdrawal reflex, blood collection was performed. The mice were then euthanized by exposure to a rising concentration of carbon dioxide, with death confirmed by cervical dislocation. The body weight of the mice at the time of cervical dislocation was 18–22 g. Pancreatic tissues were immediately fixed in 4% paraformaldehyde for subsequent histological analysis.

Histological assessment

Pancreatic tissues were dissected and immediately fixed in 4% paraformaldehyde, followed by paraffin embedding. Serial pancreatic sections (4 μm thick) were stained with hematoxylin and eosin (H&E) for histopathological evaluation. Five random fields per H&E-stained slide were selected and scored using the grading system proposed by Demol et al.[27], which evaluates abnormal architecture, acinar atrophy, fibrosis, and pseudotubular complexes. The final score was calculated as the sum of individual scores.

Pancreatic tissues from mice were subjected to immunohistochemical staining for α-smooth muscle actin (α-SMA) using a horseradish peroxidase (HRP)-based system. Two experienced pathologists independently evaluated positive staining areas. The integrated optical density (IOD) of α-SMA-positive areas was quantified using ImageJ (Full name: Image processing and Analysis in Java; Version Number: 2.0; URL Link: https://imagej.net/, USA).

Immunofluorescence staining

Pancreatic tissues from mice and CP patients were fixed in 4% paraformaldehyde, paraffin-embedded, and sectioned at a thickness of 4 μm. Sections were deparaffinized, rehydrated, and subjected to antigen retrieval using an antigen retrieval kit. After blocking with serum, sections were incubated overnight at 4 °C with primary antibodies, followed by a 1-hour incubation at room temperature with fluorophore-conjugated secondary antibodies. Nuclei were counterstained with DAPI, and a fluorescence quenching agent was applied. For dual-labeling with primary antibodies from the same species, a Tyramide Signal Amplification Kit (#G1235-100T, Servicebio) was used. Images were captured using a fluorescence microscope, and mean fluorescence intensity (MFI) was analyzed with ImageJ.

For immunofluorescence staining of primary peritoneal macrophages and pancreatic stellate cells, cell culture slides were used. Briefly, slides were pre-placed in 6-well plates, followed by the addition of peritoneal lavage fluid (for macrophages) or medium containing isolated and cultured pancreatic stellate cells (for stellate cells). After 2 h of incubation for peritoneal macrophages and 24 h for PSCs, non-adherent cells were removed. The cells adherent to the slides were considered peritoneal macrophages or PSCs, respectively. Following respective treatments, both cell types were processed for staining using the method described above,.

Measurement of IL-18 and IL-4

Peripheral blood was collected from patients with CP and murine models, along with supernatant samples from pancreatic acinar cell cultures. Blood samples were stored overnight at 4 °C and centrifuged at 3,000 rpm for 10 min to isolate serum. For tissue processing, thawed tissues were placed on ice and homogenized in lysis buffer containing protease inhibitors using a tissue grinder. The homogenates were incubated on ice, then centrifuged at 4 °C and 13,000 rpm for 15 min. The resulting supernatant is collected for subsequent ELISA experiments. Levels of IL-18 (#GEM0010, Servicebio) and IL-4 (#GEM0008, Servicebio) were measured using commercial ELISA kits according to the manufacturer's instructions. Absorbance was read using a microplate reader (Rayto RT-6100, China).

Fibrosis assessment

The extent of PF was evaluated using Masson trichrome staining. Tissue sections were sequentially stained with Masson A, B, C, D, E, and F solutions according to the manufacturer's protocol, followed by differentiation with 1% glacial acetic acid, rapid dehydration, and sealing with neutral mounting medium. After staining, sections were examined under a microscope, and fibrotic areas were identified as blue-stained regions. The percentage of fibrotic area was quantified using ImageJ.

Mouse PSCs isolation and intervention

PSCs were isolated from the pancreata of C57BL/6J and *Il-18rα*$^{-/-}$ mice. Briefly, pancreatic tissues were rinsed with Gey's balanced salt solution, minced, and digested with collagenase P (#C9407, Sigma-Aldrich). PSCs were then separated via density gradient centrifugation. The isolated PSCs were cultured in DMEM/F12 medium supplemented with 10% fetal bovine serum and 1% penicillin/streptomycin. After 24 h of culture, the medium was replaced, and cells were maintained for an additional 72 h before experimentation.

To investigate the effects of IL-18 on PSCs, cells were treated with recombinant murine IL-18 (rmIL-18; HY-P73181, MedChemExpress). Following 72 h of culture, PSCs were exposed to varying concentrations of rmIL-18 (0 or 100 ng/mL) in serum-free medium for 24 h. RNA and protein were subsequently extracted for quantitative PCR (qPCR) and Western blot analyses to assess the expression of target genes.

Mouse peritoneal macrophage isolation and intervention

Peritoneal macrophages were isolated from C57BL/6 and *Il-18rα*$^{-/-}$ mice using previously described methods[28]. Briefly, mice received an intraperitoneal injection of 3% thioglycollate broth (#70157, Sigma-Aldrich). After 72 h, mice were euthanized, and 10 mL of PBS was injected intraperitoneally to harvest peritoneal exudate cells. The cells were centrifuged at 1,000 rpm for 5 min, resuspended, and subjected to red blood cell lysis. The remaining cells were plated in 6-well plates and cultured in 2 mL RPMI 1640 medium supplemented with 10% fetal bovine serum and 1% penicillin/streptomycin. After overnight incubation, non-adherent cells were removed, and the adherent cells were defined as peritoneal macrophages.

To investigate the effects of IL-18-treated PSCs on macrophages, conditioned medium from PSCs under different treatment conditions was added to macrophages for 24-hour co-culture, including comparative groups with rabbit anti-mouse IL-4 neutralizing antibody (5 μg/mL) and rabbit IgG as an isotype control, a control group with direct IL-18 intervention on PSCs was also included. Macrophage polarization was assessed using quantitative PCR, immunofluorescence, and Western blot.

Isolation of mouse PACs and the Preparation of conditioned medium

Pancreatic acinar cells were isolated using established methods[29,30]. Briefly, the freshly collected pancreas was digested with collagenase IV (40510ES60, Yeasen) in the presence of 0.1 mg/mL soybean trypsin inhibitor (T6414, Sigma, USA). The digested tissue was filtered through a 100 μm cell strainer and further purified by sedimentation in DMEM containing 4% bovine serum albumin. The cells were then resuspended in DMEM supplemented with 0.1 mg/mL soybean trypsin inhibitor and 1% BSA, and seeded into 6-well plates.

To induce acinar cell injury, cells were treated with Cholecystokinin (CCK) (100 nM) for 30 min, while the control group received an equal volume of PBS. After treatment, the medium was replaced with fresh medium, and the cells were cultured for an additional 6 h. The supernatant was subsequently collected for ELISA.

RNA extraction and quantitative Real-Time PCR

Total RNA was extracted from primary PSCs and peritoneal macrophages using an RNA extraction kit (#AG21024, Accurate Biotech) following the manufacturer's instructions. RNA purity and concentration were analyzed using a NanoDrop 2000 spectrophotometer (Thermo Fisher Scientific). cDNA was synthesized using HiScript II Q RT SuperMix (#R223, Vazyme Biotech Co., Ltd.). Quantitative real-time PCR was performed using Q1 SYBR qPCR Master Mix (#22201, Tolo Biosciences). Primer sequences are listed in Supplementary Table 1.

Western blotting

Primary peritoneal macrophages were lysed in ice-cold RIPA buffer containing protease inhibitors (#BL612A, Biosharp) and phosphatase inhibitors (#BL615A, Biosharp) for 20 min. Lysates were centrifuged at 13,000 rpm for 15 min at 4 °C to collect proteins. Protein concentration was determined using a BCA protein assay kit (#G2026, Servicebio). Proteins were denatured, separated by SDS-PAGE, and transferred to a PVDF membrane (#GVWP04700, Millipore). The membrane was blocked with 7% skimmed milk for 1 h, incubated with primary antibodies overnight at 4 °C, and then with species-matched secondary antibodies for 1 h at room temperature. Protein bands were visualized using chemiluminescent substrate (#BL520A, Biosharp), and relative expression levels were quantified with ImageJ software.

Statistical analysisS

All data are presented as mean ± standard deviation (SD) from at least three independent experiments or animals. Statistical analyses were performed using GraphPad Prism 8 software (Full name: GraphPad Prism; Version Number: 8.0; URL Link: https://www.graphpad.com/, USA). The associations between two continuous variables were evaluated by Pearson's correlation analysis. Comparisons between two groups were analyzed using a two-tailed Student's t-test. Multiple comparisons were assessed by one-way ANOVA followed by Dunnett's post hoc test. A p-value < 0.05 was considered statistically significant.

Results

IL-18 expression in CP pancreatic tissues positively correlates with pancreatic PF

Considering the potential roles of IL-18 in fibrotic diseases, we evaluated IL-18 as a possible mediator connecting to PF. Immunofluorescence staining was performed on pancreatic tissues obtained from CP patients undergoing surgery and on normal pancreatic tissues from non-CP surgical controls. Compared to normal tissues, IL-18 expression was significantly increased in CP samples. Amylase—a marker of PACs—was markedly elevated in CP tissues and showed significant co-localization with IL-18, indicating that PACs are the one of the major sources of IL-18 in CP (Fig. 1A). Similarly, IL-18Rα expression was significantly upregulated in CP tissues (Fig. 1B). Serum IL-18 in CP patients was considerably higher than that in non-CP controls (Fig. 1C). H&E staining confirmed typical pathological changes in CP. At the same time, Masson staining revealed extensive fibrotic areas (Fig. 1D). Pancreatic tissue homogenates from CP patients also displayed significantly higher IL-18 levels compared to controls (Fig. 1E). Importantly, IL-18 concentrations in tissue homogenates were positively correlated with the extent of pancreatic fibrosis within the same patient-derived samples ($R^2 = 0.68$, $P = 0.0223$) (Fig. 1F). To verify that primary PACs are one of the major sources of IL-18, we isolated PACs in vitro and found that CCK stimulation induced PACs injury and was accompanied by IL-18 release into the culture supernatant (Fig. 1G).

IL-18Rα knockout attenuates PF, PSC activation, and M2 macrophage infiltration

To determine the functional consequences of elevated IL-18 in CP, CP models were established in WT and *Il-18rα*$^{-/-}$ mice via repeated caerulein injections for 6 weeks. Significant CP-like pathological alterations were observed in both WT and *Il-18rα*$^{-/-}$ mice following caerulein treatment, as revealed by histological analysis via H&E staining. However, total histopathological scores were markedly reduced in *Il-18rα*$^{-/-}$ mice compared with WT CP models, encompassing acinar-to-ductal metaplasia, loss of acinar parenchyma, and stromal fibrosis (Fig. 2A, B). Consistently, Masson trichrome staining further confirmed a substantial reduction in fibrotic areas in *Il-18rα*$^{-/-}$ mice (Fig. 2A, C). Expression of α-SMA, a hallmark of activated PSCs[4], was significantly downregulated in pancreatic tissues of *Il-18rα*$^{-/-}$ mice, as demonstrated by immunohistochemical staining (Fig. 2A, D). The progression and resolution of pancreatitis are critically influenced by macrophage polarization, ultimately shaping disease outcomes[31]. Notably, IL-18Rα deficiency was associated with a pronounced increase in pro-inflammatory M1 macrophage infiltration (marked by inducible nitric oxide synthase, iNOS) (Fig. 2E, F) and a concurrent decrease in reparative M2 macrophages (marked by CD206) (Fig. 2G, H).

IL-18Rα is primarily expressed on PSCs in CP pancreatic tissues

Our previous findings identified PACs as a major source of IL-18 in CP. To further elucidate the cellular localization of IL-18 binding to its receptor IL-18Rα in both human and murine CP, immunofluorescence

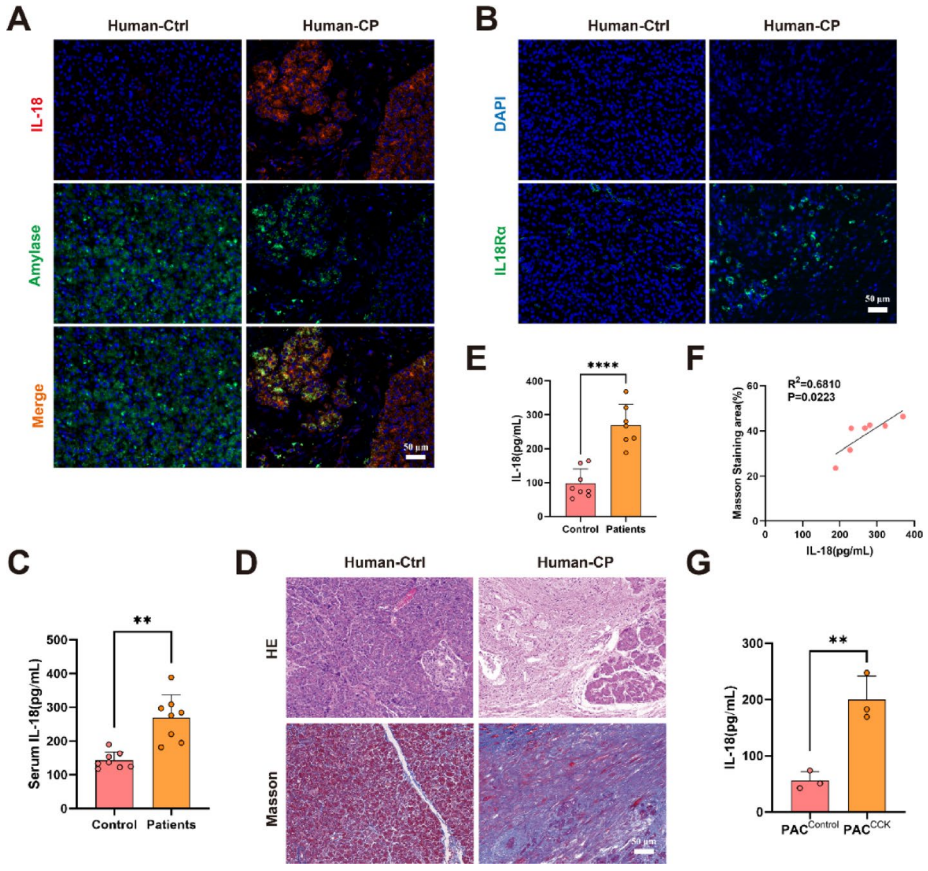

Fig. 1. IL-18 expression in CP pancreatic tissues positively correlates with PF. **(A)** Immunofluorescence staining showed IL-18 expression and co-localization with acinar cells in human CP tissues compared to the normal pancreas ($n = 6$). **(B)** IF for IL-18Rα in CP tissues ($n = 6$). **(C)** Serum IL-18 concentrations in CP patients and controls measured by ELISA ($n = 8$). **(D)** Histopathology (H&E) and fibrosis assessment by Masson's trichrome ($n = 7$). **(E)** IL-18 levels in pancreatic tissue homogenates from CP and normal samples ($n = 7$–8). **(F)** Correlation analysis between tissue IL-18 expression and the fibrotic area in the same patient ($n = 7$). (**G**) IL-18 levels in PACs supernatants after CCK treatment. Data are mean ± SEM. ns, not significant, $^{*}P < 0.05$, $^{**}P < 0.01$, $^{***}P < 0.001$, $^{****}P < 0.0001$. Scale bar = 50 μm. Ctrl control, CP chronic pancreatitis. PACs pancreatic acinar cells. CCK Cholecystokinins.

staining was performed. A significant increase in macrophage infiltration (marked by F4/80 in mice and CD68 in humans) was observed in CP tissues compared with standard controls. However, IL-18Rα expression exhibited minimal colocalization with these macrophage markers (Fig. 3A, B). Of note, IL-18Rα exhibited pronounced colocalization with α-SMA, a definitive marker of PSCs, indicating that IL-18Rα is predominantly localized to PSCs in CP pancreatic tissues (Fig. 3C, D).

IL-18 promotes IL-4 secretion by PSCs

Direct in vitro stimulation of macrophages with IL-18 has been reported to fail to induce M2 polarization, suggesting that IL-18 promotes macrophage M2 polarization through an indirect mechanism[32]. Given the critical role of IL-4 in driving M2 polarization[21,33], we hypothesized that IL-18 enhances this process by stimulating IL-4 secretion from PSCs. To test this, the localization of IL-4 and α-SMA in human CP tissues was assessed. Significantly elevated IL-4 expression was detected in CP samples, with pronounced co-localization between IL-4 and α-SMA, thereby confirming PSCs are a major source of IL-4 (Fig. 4A, C). In accordance with these findings, IL-4 levels were markedly reduced in *Il-18rα*$^{-/-}$ mice (Fig. 4B, D). To further validate this mechanism, primary PSCs isolated from WT mice were treated with rmIL-18 (Fig. 4E), the purity of the extracted PSCs was evaluated by immunofluorescence detection of α-SMA, and statistical analysis showed a purity of (97.16 ± 1.70)% (Fig. 4F). Compared with untreated controls, rmIL-18 treatment significantly upregulated IL-4 mRNA expression in PSCs and increased IL-4 protein levels in PSC supernatants (Fig. 4G, H); however, it did not considerably alter the mRNA levels of α-SMA and TGF-β1 (Fig. 4G). In addition, the Western blot results showed that IL-18 did not directly increase collagen I expression in PSCs (Fig. 4I). These findings indicate that IL-18 directly stimulates IL-4 secretion from PSCs.

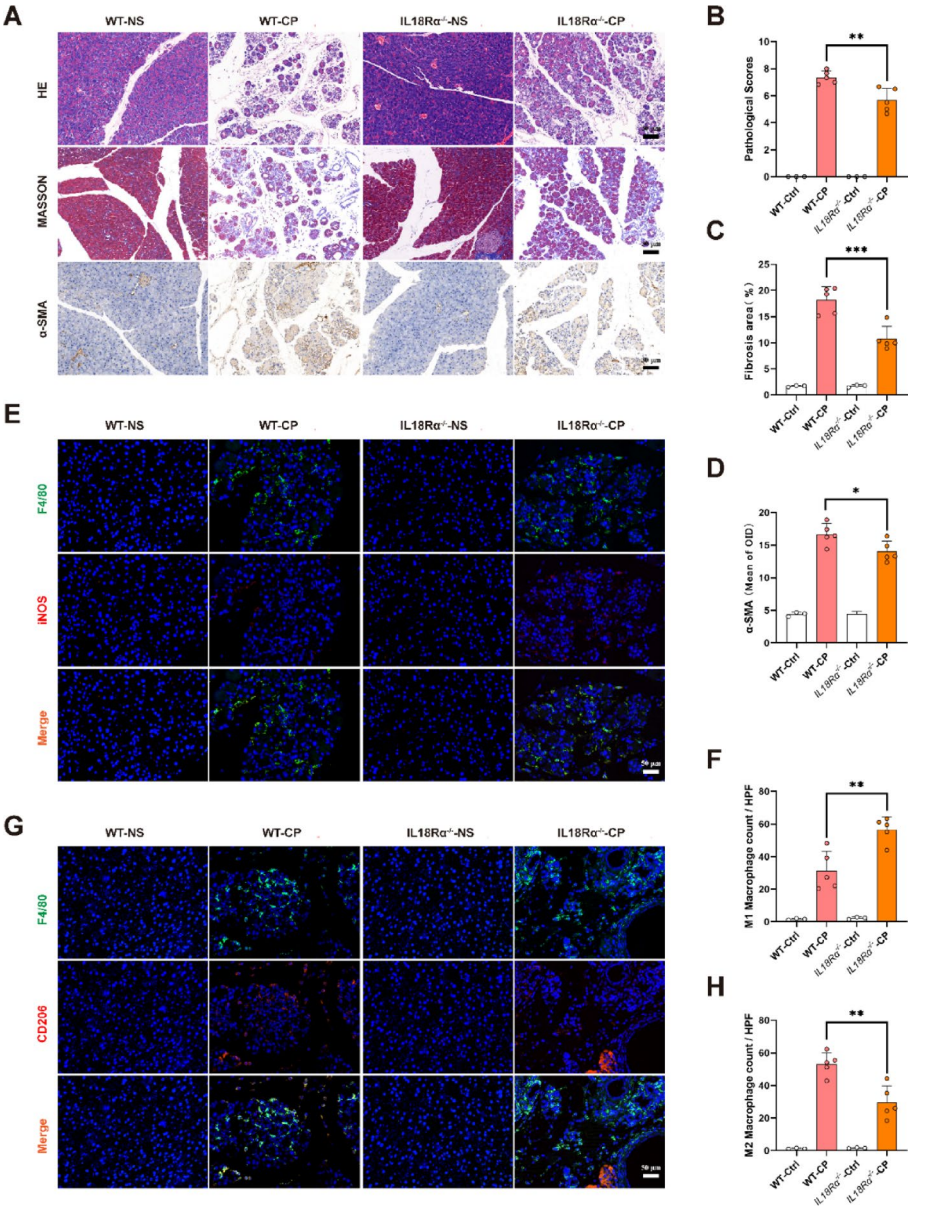

Fig. 2. IL-18Rα knockout mitigates PF, PSC activation, and M2 macrophage infiltration. **(A - D)** H&E and Masson's trichrome staining of pancreata from WT and *Il-18rα-/-* mice after caerulein-induced CP, with composite histopathology scores (architecture, acinar atrophy, fibrosis, pseudotubular complexes) and quantification of fibrotic area; α-SMA IHC for PSC activation ($n = 3–5$). Scale bar = 30 μm. **(E - H)** IF analysis of macrophage polarization markers (iNOS for M1, CD206 for M2) in normal and CP tissues of both genotypes ($n = 3–5$). Data are mean ± SEM. ns, not significant, $^{*}P < 0.05$, $^{**}P < 0.01$, $^{***}P < 0.001$, $^{****}P < 0.0001$. Scale bar = 50 μm. NS normal saline, CP chronic pancreatitis.

IL-18 drives M2 macrophage polarization via PSC-derived IL-4

To investigate the functional impact of PSC-derived IL-4 on macrophages, primary PSCs and peritoneal macrophages were isolated from WT mice. PSCs were treated with varying concentrations of rmIL-18 or an IL-4-neutralizing antibody, and conditioned media from these PSCs were used to treat pre-plated macrophages (Fig. 5A). CD206 expression in macrophages was significantly increased by conditioned media from IL-18-stimulated PSCs, indicating M2 polarization. This effect was substantially reduced by IL-4 inhibition (Fig. 5B). The Western blot results showed that rmIL-18 alone was unable to directly induce M2 polarization in macrophages (Fig. 5C), whereas conditioned media from rmIL-18-treated PSCs significantly promoted macrophage M2 polarization. In contrast, this phenotypic effect was markedly suppressed by IL-4 neutralization (Fig. 5D). Consistent with this, qPCR analysis revealed that rmIL-18-treated PSC-conditioned media decreased mRNA levels of M1 macrophage markers while increasing mRNA levels of M2 macrophage markers. These effects were reversed by IL-4 inhibition (Fig. 5E, F).

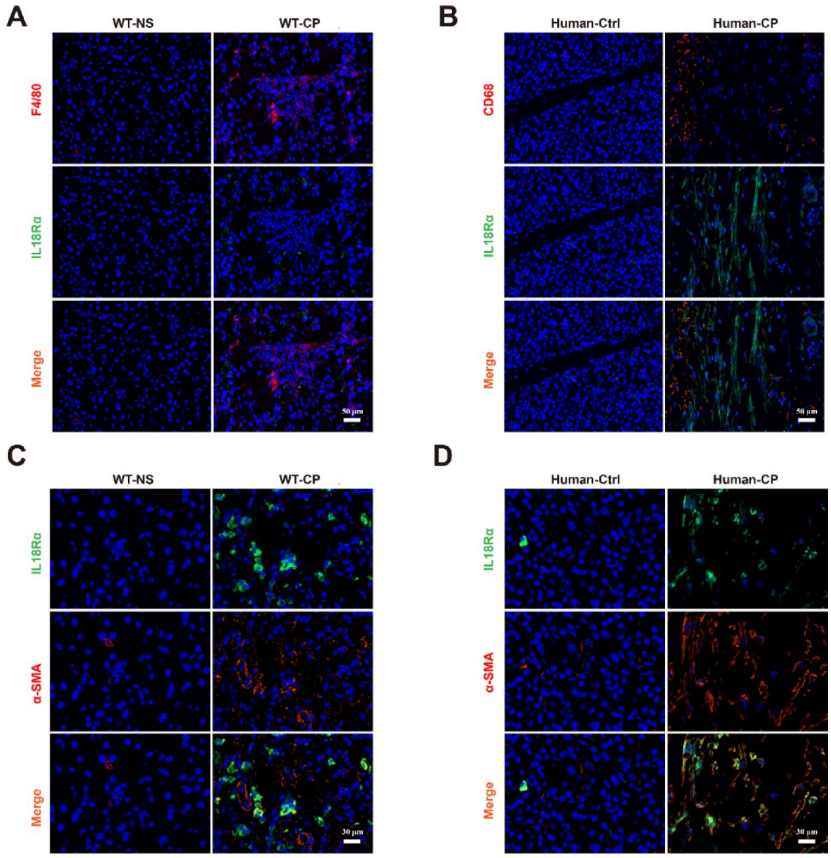

Fig. 3. IL-18Rα is predominantly expressed on PSCs in CP pancreatic tissues. **(A, B)** IF assessed macrophage infiltration in murine CP tissues. Co-localization of IL-18Rα with macrophage markers (F4/80 for murine tissues, CD68 for human tissues) to determine its cellular expression ($n = 3$). Scale bar = 50 μm. **(C, D)** Co-localization of IL-18Rα with the PSC marker α-SMA was examined in both murine and human CP tissues ($n = 3$). Scale bar = 30 μm. NS normal saline, CP chronic pancreatitis, Ctrl control.

To validate the in vivo relevance of the above findings, we injected rmIL-18, along with an IL-4 inhibitor, during CP model establishment in wild-type mice. The results showed that rmIL-18 treatment alone did not induce morphological changes in pancreatic tissue. However, under CP conditions, mice treated with rmIL-18 exhibited a significant exacerbation of CP severity, characterized by increased pancreatic parenchymal cell death, fibrotic proliferation, abnormal tissue architecture, and acinar ductal metaplasia. Masson's trichrome staining confirmed a marked increase in fibrotic area, along with elevated IL-4 expression. Importantly, the effects of rmIL-18 in the CP model were significantly attenuated upon IL-4 inhibition (Fig. 6A). Subsequent analysis of macrophage polarization was consistent with the in vitro results: rmIL-18 administration in the CP model led to increased infiltration of M2-type macrophages, while IL-4 inhibition reduced M2 macrophage infiltration, further supporting the role of the IL-18/IL-4 axis in driving macrophage M2 polarization in chronic pancreatitis (Fig. 6B, C).

Discussion

CP is characterized by persistent inflammation and PF, driven by dynamic crosstalk among injured PACs, PSCs, and immune cells. Inflammasome-associated pathways have been implicated in acinar injury during CP, and IL-18 is a key downstream cytokine linked to fibrotic responses in multiple organs[10,34,35]. In this study, we observed consistent upregulation of IL-18 in human CP tissues and murine CP models, with IL-18 levels correlating with fibrosis severity. Genetic disruption of IL-18Rα markedly attenuated pancreatic injury, PSC activation, M2-skewing macrophage responses, and fibrosis, supporting a functional role for IL-18/IL-18Rα signaling in PF.

To elucidate how IL-18 promotes PF, we investigated IL-18Rα expression in CP samples. Our results showed that IL-18Rα is predominantly localized in PSCs, indicating that IL-18 may directly modulate PSC function to drive fibrotic processes. This observation extends the prevailing view that IL-18 acts largely within immune compartments by suggesting that PSCs may also represent an important IL-18–responsive stromal target in CP[11,36,37]. Given the pivotal role of PSC activation in PF, the finding that IL-18 activates hepatic stellate cells, and our observation that IL-18 signaling deficiency significantly suppresses PSC activation. We therefore next asked whether IL-18 modulates PSC activation in CP. Although adding rmIL-18 directly to PSCs in vitro did not lead to an upregulation of α-SMA or changes in collagen I in our study, which differs to some extent from previous reports, this discrepancy suggests that IL-18–mediated stellate cell activation may be organ-specific[34].

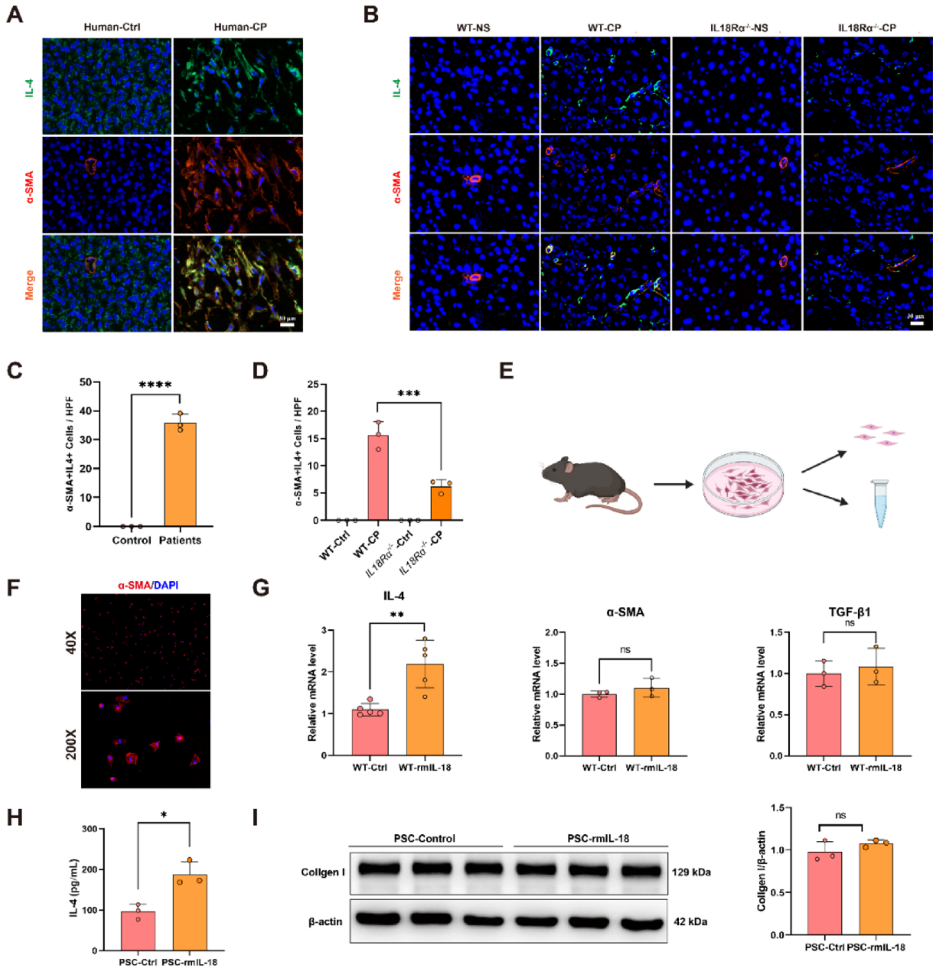

Fig. 4. IL-18 promotes IL-4 secretion by PSCs. **(A, C)** IF of human CP tissues showed IL-4 expression and co-localization with α-SMA ($n = 6$). **(B, D)** Reduced pancreatic IL-4 expression in normal and chronic pancreatic tissues of both genotypes ($n = 3–5$). **(E)** Schematic of primary murine PSC isolation and stimulation. **(F)** The purity of the extracted PSCs was evaluated by immunofluorescence detection of α-SMA. **(G)** PSCs were treated with rmIL-18, and qPCR was used to detect changes in the expression of IL-4, α-SMA, and TGF-β1 ($n = 5$). **(H)** ELISA was used to measure changes in the IL-4 protein levels in the culture supernatant of PSCs treated with rmIL-18 ($n = 3$). **(I)** Western blot results of PSCs after intervention Data are mean ± SEM. ns, not significant, $^{*}P < 0.05$, $^{**}P < 0.01$, $^{***}P < 0.001$, $^{****}P < 0.0001$. Scale bar = 30 μm. NS normal saline, Ctrl control, CP chronic pancreatitis. PSC pancreatic stellate cells.

It also indicates that PSC activation is likely driven by multiple cell types and microenvironmental cues, and the precise role of IL-18 in this process warrants further investigation. In addition, our current study revealed that a deficiency in IL-18 signaling significantly reduces M2 macrophage infiltration, suggesting that IL-18-mediated regulation of macrophage polarization occurs indirectly, via PSCs as an intermediate hub.

Macrophages play a central role in the immune microenvironment of CP. They are not only critical in immune surveillance but also regulate inflammatory responses and tissue repair through distinct polarization states. In CP, M2 macrophages were verified to activate PSCs through the production of TGF-β and PDGF-β, potentially driving CP pathogenesis[38,39]. Additionally, M2 macrophages regulate pancreatic cell turnover, influence metabolism, and shape the immune microenvironment, all of which contribute to disease progression. Moreover, previous studies have reported that IL-18 deficiency inhibits M2 macrophage polarization in cardiac and renal fibrosis. However, the precise molecular mechanisms underlying this inhibitory effect remain unclear. Our experimental results demonstrate that IL-18 fails to promote M2 polarization of macrophages in vitro but directly stimulates PSCs to secrete IL-4, and PSC-derived IL-4 is a key mediator driving M2 macrophage polarization. This mechanism was validated both in vitro and in vivo: Conditioned medium from IL-18-treated PSCs significantly upregulated M2 macrophage markers, an effect abolished by IL-4 neutralization. Furthermore, Xue J et al.[21] demonstrated that IL-4 promotes the progression of CP by inducing M2 macrophage polarization, and the inhibition of IL-4 was shown to reduce PF. PSCs were identified as a source of IL-4. These findings support a model "IL-18→PSCs→IL-4→M2 macrophage polarization" signaling cascade, explaining how the inflammatory microenvironment in CP promotes fibrosis through intercellular crosstalk. Importantly, inhibition of IL-4 significantly attenuates the profibrotic effect of exogenous IL-18 administration on CP progression, indicating

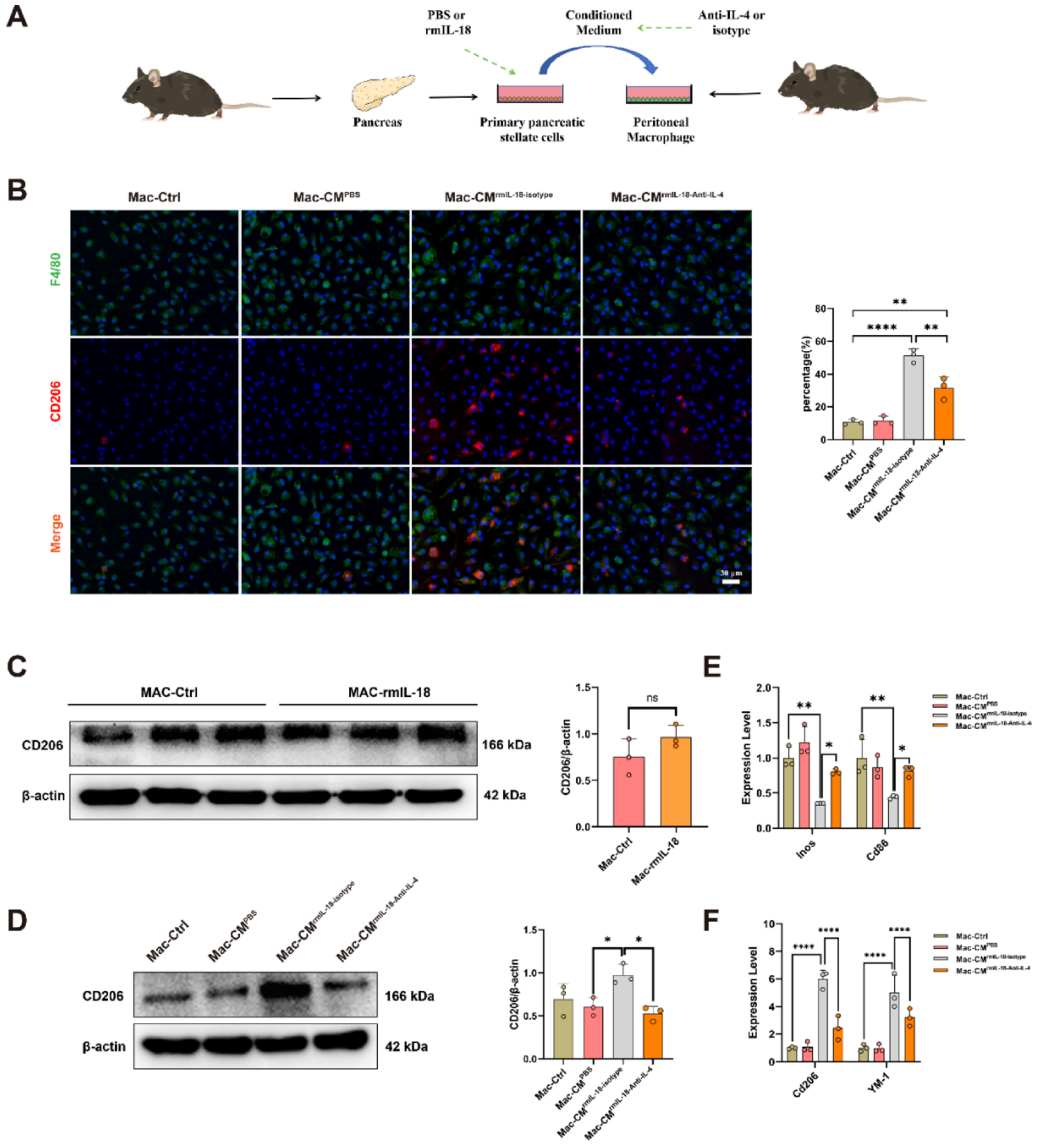

Fig. 5. IL-18 drives M2 macrophage polarization via PSC-derived IL-4. **(A)** PSCs were cultured with or without rmIL-18, and then CM from different conditions were added to peritoneal macrophages seeded in plates. **(B)** The polarization of macrophages treated with CM, with or without the addition of IL-4 neutralizing antibody, was evaluated ($n = 3$). **(C, D)** Western blot results of macrophages after intervention ($n = 3$). **(E, F)** Quantitative PCR analysis of transcriptional levels of canonical M1 markers (iNOS, CD86) and M2 markers (CD206, YM-1) ($n = 3$). Data are mean ± SEM. ns, not significant, $^{*}P < 0.05$, $^{**}P < 0.01$, $^{***}P < 0.001$, $^{****}P < 0.0001$. Scale bar = 30 μm. Ctrl control, Mac macrophage, CM conditioned media.

that the "PSCs→IL-4→M2 macrophage polarization" signaling axis represents a major mechanism by which IL-18 amplifies fibrotic progression in CP, while not excluding contributions from other cytokines and pathways in the in vivo inflammatory milieu. Mechanistically, IL-4 classically signals through IL-4Rα to activate JAK/STAT6-dependent transcriptional programs that drive alternative macrophage activation and profibrotic responses[40,41], suggesting that this pathway may form a positive feedback loop to perpetuate fibrotic signaling.

Although our immunofluorescence suggests that IL-4 signals are enriched in α-SMA^{+} areas, Th2 cells are canonical IL-4 producers and should been considered in the exploration of source of IL-4 expressed in the pancreatic tissue with CP. However, recent research has indicated that IL-4 was expressed in certain Th2 cells in pancreatic tissue with CP, but Th2 cells accounted for only approximately 5% of CD4 + cells infiltrated in pancreatic tissue with CP[42], so we didn't detect the expression of IL-4 in Th2 cells and focused on exploring the role of PSC-derived IL-4. For this purpose, we performed immune-cell–free in vitro experiments which demonstrate that purified primary PSCs can secrete IL-4 upon IL-18 stimulation and IL-4 released by IL-18-treated PSCs can promote M2 macrophage polarization, supporting PSCs as an important stromal source of IL-4 in this pathway. However, we still cannot formally exclude CD3^{+}/CD4^{+} T cells as additional contributors to the bulk IL-4 pool in CP tissue. Future studies incorporating IL-4 co-staining with CD3/CD4 and quantitative

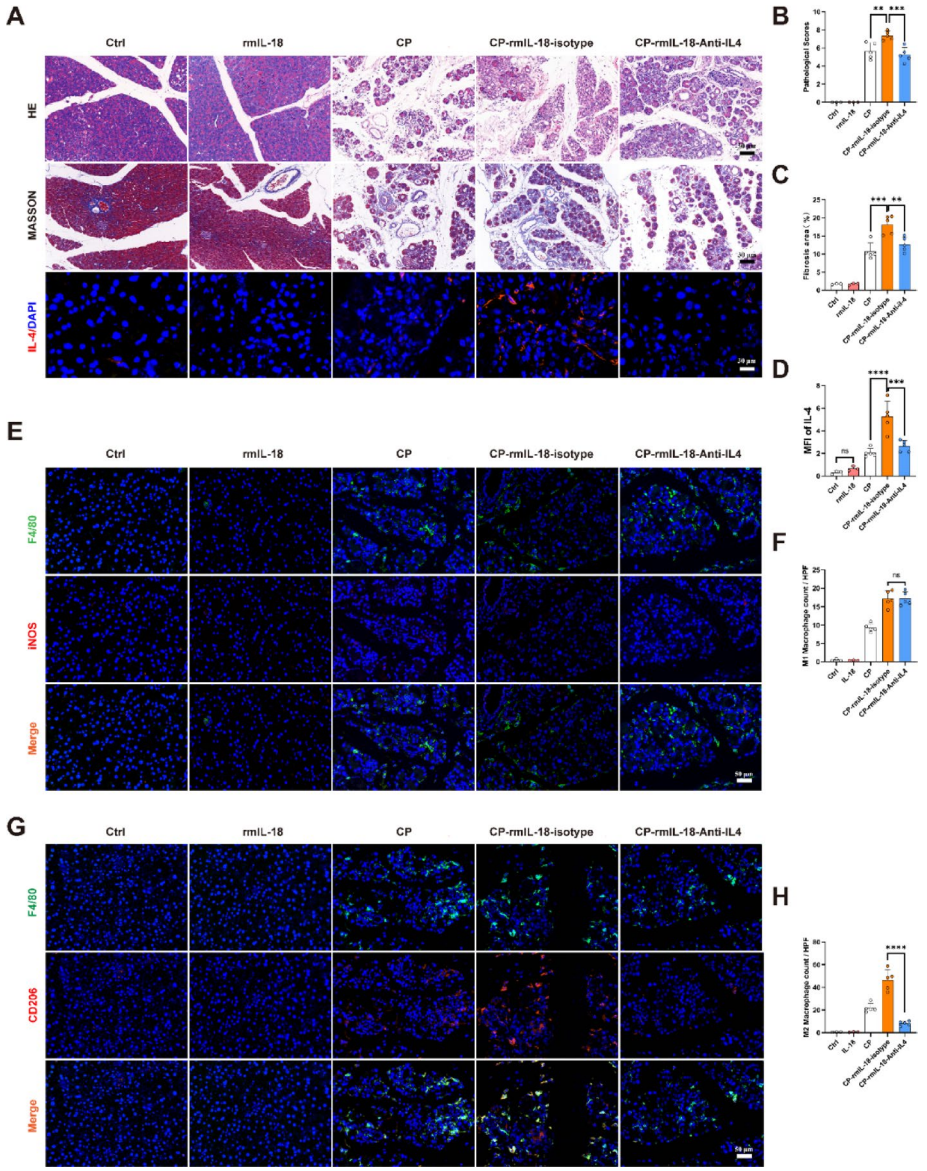

Fig. 6. IL-18 exacerbates CP severity in vivo via the IL-4/M2 axis. **(A)** WT mice with caerulein-induced CP received rmIL-18 with or without IL-4 neutralizing antibody. H&E and Masson's trichrome staining images with fibrosis quantification; pancreatic IL-4 assessed by IF ($n = 3–5$). Scale bar = 30 μm **(B, C)** IF analysis of macrophage polarization markers in macrophages treated with rmIL-18, with or without IL-4 inhibition. ($n = 3–5$). Data are mean ± SEM. ns, not significant, $^{*}P < 0.05$, $^{**}P < 0.01$, $^{***}P < 0.001$, $^{****}P < 0.0001$. Scale bar = 50 μm. Ctrl control, CP chronic pancreatitis.

comparisons across stromal versus immune compartments (or single-cell/spatial profiling) will be valuable for resolving the relative contributions of distinct IL-4–producing cell types in vivo.

Beyond IL-4–mediated macrophage polarization, IL-18 may also shape the inflammatory microenvironment through chemokine programs in stromal cells. IL-18 receptor signaling can activate NF-κB via a MyD88-dependent pathway[43], and NF-κB is a pivotal transcriptional hub controlling chemokine expression[44]. Consistent with this concept, IL-18 has been shown to induce chemokines such as CXCL8/IL-8 and CCL2/MCP-1 in fibroblast-like stromal cells through NF-κB/MAPK pathways[45,46]. Moreover, PSCs themselves are capable of producing chemokines (e.g., CXCL10) that can influence immune-cell recruitment[47], and IL-18 signaling can directly promote stellate-cell activation in fibrotic organs[34]. Collectively, these findings support a plausible IL-18→PSC→chemokine axis that could contribute to immune-cell recruitment into the injured pancreas and thereby facilitate fibrotic tissue remodeling. Notably, we did not directly profile chemokine secretion from IL-18–stimulated PSCs or perform chemotaxis assays in the current study; systematic chemokine profiling and in vivo validation will be important directions for future work.

Although this study provides important insights into the role of IL-18 signaling in PF, several limitations warrant further investigation. First, the CP animal models employed here rely primarily on caerulein induction,

which fails to fully recapitulate the multifactorial etiology of human CP (e.g., alcohol-associated or genetic CP). Second, we employed systemic IL-18Rα–deficient mice, which cannot distinguish the relative contributions of IL-18Rα signaling in PSCs versus macrophages or other cell types. Third, while our data support PSCs as an important stromal source of IL-4 in this axis, we did not perform IL-4 co-staining with CD3/CD4 or cell-type–resolved quantification in vivo, and immune-cell contributions to tissue IL-4 cannot be excluded. Fourth, although we used primary peritoneal macrophages as a reproducible polarization system, validation in pancreatic macrophages and/or single-cell/spatial approaches would further strengthen physiological relevance. Finally, we did not directly profile chemokine secretion from IL-18–stimulated PSCs or perform chemotaxis assays, nor did we measure canonical pyroptosis executors (e.g., GSDMD/GSDME cleavage); these experiments will be important to clarify upstream mechanisms of IL-18 release and additional IL-18–dependent stromal programs in CP.

In summary, this study elucidates a novel mechanism by which IL-18 promotes macrophage M2 polarization and PF via PSC-derived IL-4 in CP, establishing a PAC–PSC–macrophage axis and providing a rationale for therapeutic targeting of IL-18/IL-18Rα signaling and PSC–macrophage crosstalk to potentially mitigate PF in CP.

Data availability

The datasets used and/or analysed during the current study available from the corresponding author on reasonable request.

Received: 7 November 2025; Accepted: 29 January 2026
Published online: 06 February 2026

References

1. Thierens, N. et al. Chronic pancreatitis [J]. *Lancet* **404** (10471), 2605–2618 (2025).
2. Hines, O. J. & Pandol, S. J. Management of chronic pancreatitis [J]. *Bmj* **384**, e070920 (2024).
3. Saloman, J. L. et al. Characterizing mechanism-based pain phenotypes in patients with chronic pancreatitis: a cross-sectional analysis of the prospective evaluation of chronic pancreatitis for epidemiologic and translational studies [J]. *Pain* **164** (2), 375–384 (2023).
4. Wang, D. et al. Pancreatic acinar cells-Derived Sphingosine-1-Phosphate contributes to fibrosis of chronic pancreatitis via inducing autophagy and activation of pancreatic stellate cells [J]. *Gastroenterology* **165** (6), 1488–1504e1420 (2023).
5. Yang, W. J. et al. Acinar ATP8b1/LPC pathway promotes macrophage efferocytosis and clearance of inflammation during chronic pancreatitis development [J]. *Cell. Death Dis.* **13** (10), 893 (2022).
6. Gaul, S. et al. Hepatocyte pyroptosis and release of inflammasome particles induce stellate cell activation and liver fibrosis [J]. *J. Hepatol.* **74** (1), 156–167 (2021).
7. Li, Y. et al. GSDME-mediated pyroptosis promotes inflammation and fibrosis in obstructive nephropathy [J]. *Cell. Death Differ.* **28** (8), 2333–2350 (2021).
8. Liu, Y. et al. Pyroptosis in renal inflammation and fibrosis: current knowledge and clinical significance [J]. *Cell. Death Dis.* **14** (7), 472 (2023).
9. Yasuda, K., Nakanishi, K. & Tsutsui, H. Interleukin-18 in health and disease [J]. *Int. J. Mol. Sci*, **20**(3), 649 (2019).
10. Xiao, H. et al. IL-18 cleavage triggers cardiac inflammation and fibrosis upon β-adrenergic insult [J]. *Eur. Heart J.* **39** (1), 60–69 (2018).
11. Mertens, R. T. et al. A metabolic switch orchestrated by IL-18 and the Cyclic dinucleotide cGAMP programs intestinal tolerance [J]. *Immunity* **57** (9), 2077–2094 (2024). e2012.
12. Kaplanski, G. Interleukin-18: biological properties and role in disease pathogenesis [J]. *Immunol. Rev.* **281** (1), 138–153 (2018).
13. Alegre, F., Pelegrin, P. & Feldstein, A. E. Inflammasomes in liver fibrosis [J]. *Semin Liver Dis.* **37** (2), 119–127 (2017).
14. Schneider, A. et al. Enhanced expression of interleukin-18 in serum and pancreas of patients with chronic pancreatitis [J]. *World J. Gastroenterol.* **12** (40), 6507–6514 (2006).
15. Ramakrishnan, P. et al. Selective phytochemicals targeting pancreatic stellate cells as new anti-fibrotic agents for chronic pancreatitis and pancreatic cancer [J]. *Acta Pharm. Sin B.* **10** (3), 399–413 (2020).
16. Yang, X. et al. Very-low-density lipoprotein receptor-enhanced lipid metabolism in pancreatic stellate cells promotes pancreatic fibrosis [J]. *Immunity* **55** (7), 1185–1199e1188 (2022).
17. Jiang, W. et al. The pancreatic clock is a key determinant of pancreatic fibrosis progression and exocrine dysfunction [J]. *Sci. Transl Med.* **14** (664), eabn3586 (2022).
18. Lin, Y. et al. Neddylation pathway alleviates chronic pancreatitis by reducing HIF1α-CCL5-dependent macrophage infiltration [J]. *Cell. Death Dis.* **12** (3), 273 (2021).
19. Sendler, M. et al. Cathepsin B-Mediated activation of trypsinogen in endocytosing macrophages increases severity of pancreatitis in mice [J]. *Gastroenterology* **154** (3), 704–718e710 (2018).
20. Sendler, M. et al. NLRP3 inflammasome regulates development of systemic inflammatory response and compensatory Anti-Inflammatory response syndromes in mice with acute pancreatitis [J]. *Gastroenterology* **158** (1), 253–269e214 (2020).
21. Xue, J. et al. Alternatively activated macrophages promote pancreatic fibrosis in chronic pancreatitis [J]. *Nat. Commun.* **6**, 7158 (2015).
22. Watanabe, T. et al. Nucleotide-binding oligomerization domain 1 acts in concert with the cholecystokinin receptor agonist, cerulein, to induce IL-33-dependent chronic pancreatitis [J]. *Mucosal Immunol.* **9** (5), 1234–1249 (2016).
23. Tanino, A. et al. Interleukin-18 deficiency protects against renal interstitial fibrosis in aldosterone/salt-treated mice [J]. *Clin. Sci. (Lond).* **130** (19), 1727–1739 (2016).
24. Zhang, G. et al. Psidium Guajava flavonoids prevent NLRP3 inflammasome activation and alleviate the pancreatic fibrosis in a chronic pancreatitis mouse model [J]. *Am. J. Chin. Med.* **49** (8), 2001–2015 (2021).
25. Neuschwander-Tetri, B. A. et al. Repetitive acute pancreatic injury in the mouse induces Procollagen alpha1(I) expression colocalized to pancreatic stellate cells [J]. *Lab. Invest.* **80** (2), 143–150 (2000).
26. Treiber, M. et al. Myeloid, but not pancreatic, RelA/p65 is required for fibrosis in a mouse model of chronic pancreatitis [J]. *Gastroenterology* **141** (4), 1473–1485 (2011).
27. Demols, A. et al. Endogenous interleukin-10 modulates fibrosis and regeneration in experimental chronic pancreatitis [J]. *Am. J. Physiol. Gastrointest. Liver Physiol.* **282** (6), G1105–1112 (2002).
28. Wang, D. et al. YAP promotes the activation of NLRP3 inflammasome via blocking K27-linked polyubiquitination of NLRP3 [J]. *Nat. Commun.* **12** (1), 2674 (2021).

29. Zhan, X. et al. Elevated intracellular trypsin exacerbates acute pancreatitis and chronic pancreatitis in mice [J]. *Am. J. Physiol. Gastrointest. Liver Physiol.* **316** (6), G816–g825 (2019).
30. Ji, B., Kopin, A. S. & Logsdon, C. D. Species differences between rat and mouse CCKA receptors determine the divergent acinar cell response to the cholecystokinin analog JMV-180 [J]. *J. Biol. Chem.* **275** (25), 19115–19120 (2000).
31. Tan, Q. et al. YAP promotes fibrosis by regulating macrophage to myofibroblast transdifferentiation and M2 polarization in chronic pancreatitis [J]. *Int. Immunopharmacol.* **148**, 114087 (2025).
32. Kavitha, Y. & Geetha, A. Anti-inflammatory and preventive activity of white mulberry root bark extract in an experimental model of pancreatitis [J]. *J. Tradit Complement. Med.* **8** (4), 497–505 (2018).
33. Peng, C. et al. Murine chronic pancreatitis model induced by partial ligation of the pancreatic duct encapsulates the profile of macrophage in human chronic pancreatitis [J]. *Front. Immunol.* **13**, 840887 (2022).
34. Knorr, J. et al. Interleukin-18 signaling promotes activation of hepatic stellate cells in mouse liver fibrosis [J]. *Hepatology* **77** (6), 1968–1982 (2023).
35. Cui, L. et al. S1P/S1PR2 promote pancreatic stellate cell activation and pancreatic fibrosis in chronic pancreatitis by regulating autophagy and the NLRP3 inflammasome [J]. *Chem. Biol. Interact.* **380**, 110541 (2023).
36. Jaspers, J. E. et al. IL-18-secreting CAR T cells targeting DLL3 are highly effective in small cell lung cancer models [J]. *J. Clin. Invest*, **133**(9), e166028 (2023).
37. Jarret, A. et al. Enteric nervous System-Derived IL-18 orchestrates mucosal barrier immunity [J]. *Cell* **180** (1), 50–63e12 (2020).
38. Apte, M. V. et al. Pancreatic stellate cells are activated by Proinflammatory cytokines: implications for pancreatic fibrogenesis [J]. *Gut* **44** (4), 534–541 (1999).
39. Omary, M. B. et al. The pancreatic stellate cell: a star on the rise in pancreatic diseases [J]. *J. Clin. Invest.* **117** (1), 50–59 (2007).
40. Xu, Y. et al. USP25 stabilizes STAT6 to promote IL-4-induced macrophage M2 polarization and fibrosis [J]. *Int. J. Biol. Sci.* **21** (2), 475–489 (2025).
41. Shi, J. H. et al. TRAF3/STAT6 axis regulates macrophage polarization and tumor progression [J]. *Cell. Death Differ.* **30** (8), 2005–2016 (2023).
42. Glaubitz, J. et al. In mouse chronic pancreatitis CD25(+)FOXP3(+) regulatory T cells control pancreatic fibrosis by suppression of the type 2 immune response [J]. *Nat. Commun.* **13** (1), 4502 (2022).
43. Adachi, O. et al. Targeted disruption of the MyD88 gene results in loss of IL-1- and IL-18-mediated function [J]. *Immunity* **9** (1), 143–150 (1998).
44. Liu, T. et al. NF-κB signaling in inflammation [J]. *Signal. Transduct. Target. Ther.* **2**, 17023 (2017).
45. Morel, J. C. et al. Interleukin-18 induces rheumatoid arthritis synovial fibroblast CXC chemokine production through NFkappaB activation [J]. *Lab. Invest.* **81** (10), 1371–1383 (2001).
46. Amin, M. A. et al. Interleukin-18 induces angiogenic factors in rheumatoid arthritis synovial tissue fibroblasts via distinct signaling pathways [J]. *Arthritis Rheum.* **56** (6), 1787–1797 (2007).
47. Lunardi, S. et al. IP-10/CXCL10 induction in human pancreatic cancer stroma influences lymphocytes recruitment and correlates with poor survival [J]. *Oncotarget* **5** (22), 11064–11080 (2014).

Author contributions

G.T. and Z.L. designed the experiment and analyzed the data. G.T. and H.J. performed the research and wrote the manuscript. C.P. and S.X. assisted in completing the experiment. S.Z. and L.C. reviewed and modified the manuscript. Z.L. and X.Y. provided overall guidance and supervision.

Funding

The current study was funded by the National Natural Science Foundation of China (No. 82100688 and 82472226). Natural Science Foundation of Hunan Province (No. 2022JJ40740).

Declarations

Competing interests

The authors declare no competing interests.

Additional information

Supplementary Information The online version contains supplementary material available at https://doi.org/10.1038/s41598-026-38168-5.

Correspondence and requests for materials should be addressed to Z.L.